

NNLO predictions for the Higgs boson signal in the $H \rightarrow WW \rightarrow l\nu l\nu$ and $H \rightarrow ZZ \rightarrow 4l$ decay channels

Massimiliano Grazzini

INFN, Sezione di Firenze,
I-50019 Sesto Fiorentino, Florence, Italy

Abstract

We consider Standard Model Higgs boson production by gluon–gluon fusion in hadron collisions. We present a calculation of the next-to-next-to-leading order QCD corrections to the cross section in the $H \rightarrow WW \rightarrow l\nu l\nu$ and $H \rightarrow ZZ \rightarrow 4l$ decay channels. The calculation is implemented in the parton level Monte Carlo program **HNNLO** and allows us to apply arbitrary cuts on the final state leptons and the associated jet activity. We present selected numerical results for the signal cross section at the LHC, by using all the nominal cuts proposed for the forthcoming Higgs boson search.

1 Introduction

The search for the Higgs boson [1] and the study of its properties (mass, couplings, decay widths) are at the heart of the LHC physics program. In this paper we consider the production of the Standard Model (SM) Higgs boson by the gluon fusion mechanism.

The gluon fusion process $gg \rightarrow H$, through a heavy-quark (mainly, top-quark) loop, is the main production mechanism of the SM Higgs boson H at hadron colliders. When combined with the decay channels $H \rightarrow \gamma\gamma$, $H \rightarrow WW$ and $H \rightarrow ZZ$, this production mechanism is one of the most important for Higgs boson searches and studies over the entire range, $100 \text{ GeV} \lesssim M_H \lesssim 1 \text{ TeV}$, of Higgs boson mass M_H to be investigated at the LHC [2, 3].

The dynamics of the gluon fusion mechanism is controlled by strong interactions. Detailed studies of the effect of QCD radiative corrections are thus necessary to obtain accurate theoretical predictions.

At leading order (LO) in QCD perturbation theory, the cross section is proportional to α_s^2 , α_s being the QCD coupling. The QCD radiative corrections to the total cross section have been computed at the next-to-leading order (NLO) in Refs. [4, 5, 6] and found to enhance the cross section by about 80 – 100%. In recent years also the next-to-next-to-leading order (NNLO) corrections [7, 8, 9, 10, 11, 12] have been computed. The NNLO effect is moderate and, for a light Higgs, it increases the NLO cross result by about 15 – 20%. The effects of a jet veto on the total cross section has also been studied up to NNLO [13]. We recall that all the NNLO results have been obtained by using the large- M_t approximation, M_t being the mass of the top quark.

The NNLO results mentioned above are certainly important, but they refer to situations where the experimental cuts are either ignored (as in the case of the total cross section) or taken into account only in simplified cases (as in the case of the jet vetoed cross section). Generally speaking, the impact of higher-order corrections may be strongly dependent on the details of the applied cuts and also the shape of the distributions is typically affected by these details.

The first NNLO calculation that fully takes into account experimental cuts was reported in Ref. [14], in the case of the decay mode $H \rightarrow \gamma\gamma$. In Ref. [15] the calculation is extended to the decay mode $H \rightarrow WW \rightarrow l\nu l\nu$.

In Ref. [16] we have presented an independent NNLO calculation of the Higgs production cross section, including the decay $H \rightarrow \gamma\gamma$. The method is completely different from that used in Refs. [14, 15]. Our calculation is based on the *subtraction method*.

The subtraction method [17] is probably the most popular technique to handle and cancel infrared singularities in QCD computations at high energy, and has lead to the formulation of general algorithms [18, 19] to perform NLO calculations in a relatively straightforward manner, once the relevant amplitudes are available. In recent years, several research groups have been working to develop general NNLO extensions of the subtraction method [20, 21, 22, 23, 24]. NNLO results, however, have been obtained only in some specific processes. The calculation of $e^+e^- \rightarrow 2 \text{ jets}$ [25, 26] was the first to be addressed, and, more recently, the computation of $e^+e^- \rightarrow 3 \text{ jets}$ [27, 28, 29] has been completed.

The version of the subtraction method proposed in Ref. [13] can be applied to a specific

class of processes, namely, the production of colourless high-mass systems (lepton pairs, vector bosons, Higgs bosons, ...) in hadron collisions. As usual for calculations performed within the subtraction formalism, the computation can be organized into a parton level event generator. The latter feature is particularly useful, since the user can apply the required cuts on the final state and plot the corresponding distributions in the form of bin histograms.

In Ref. [16] we have applied our method to the computation of the Higgs production cross section, including the decay $H \rightarrow \gamma\gamma$. In the present paper we extend the calculation of Ref. [16] to the other important decay modes of the Higgs boson, namely, $H \rightarrow WW \rightarrow l\nu l\nu$ and $H \rightarrow ZZ \rightarrow 4$ leptons, and present predictions for the Higgs boson signal that take into account all the realistic experimental cuts on the final state leptons and the associated jet activity.

The paper is organized as follows. In Sect. 2 we describe our NNLO Monte Carlo program. In Sect. 3 we present the results of our calculation for the decay modes $H \rightarrow WW \rightarrow l\nu l\nu$ and $H \rightarrow ZZ \rightarrow 4l$. In Sect. 4 we summarize our results.

2 The HNNLO Monte Carlo program

The numerical program **HNNLO** is a fortran code that implements the version of the subtraction method proposed in Ref. [16]. The program computes the Higgs boson production cross section at hadron colliders up to NNLO in QCD perturbation theory.

The cross section up to (N)NLO can be written as

$$d\sigma_{(N)NLO}^H = \mathcal{H}_{(N)NLO}^H \otimes d\sigma_{LO}^H + \left[d\sigma_{(N)LO}^{H+jets} - d\sigma_{(N)LO}^{CT} \right] . \quad (1)$$

The first term (*virtual*) is the simplest to compute numerically: it contains the LO cross section $d\sigma_{LO}^H$ at $q_T = 0$, q_T being the transverse momentum of the Higgs boson, suitably convoluted with a hard function \mathcal{H} which includes the regularized one-loop (two-loop) corrections to the LO process. The second term (*real*) is the most cumbersome to evaluate. Its first contribution, $d\sigma_{(N)LO}^{H+jets}$, is the (N)LO cross section for the production of the Higgs boson in association with one (or more) jets. This contribution is evaluated with the version of the subtraction method of Ref. [19], as implemented in the MCFM [30] package. When $q_T \rightarrow 0$, $d\sigma_{(N)LO}^{H+jets}$ is divergent, and is supplemented with the subtraction of a suitable counterterm, $d\sigma_{(N)LO}^{CT}$. The difference in the square bracket of Eq. (1) is thus finite as $q_T \rightarrow 0$.

In the present version of the code (version 1.1) we have implemented three decay modes for the Higgs boson: $H \rightarrow \gamma\gamma$ [16], $H \rightarrow WW \rightarrow l\nu l\nu$ [†] and $H \rightarrow ZZ \rightarrow 4$ leptons. In the latter case the user can choose between $H \rightarrow ZZ \rightarrow \mu^+\mu^-e^+e^-$ and $H \rightarrow ZZ \rightarrow e^+e^-e^+e^-$, which includes the appropriate interference contribution. The program can be downloaded from [31], together with some accompanying notes.

[†]Results for this decay channel were presented at the Les Houches Workshop “Physics at TeV Colliders” in June 2007, and at the Radcor Conference in October 2007.

3 Results up to NNLO

3.1 Preliminaries

We consider Higgs boson production at the LHC (e.g. pp collisions at $\sqrt{s} = 14$ TeV). We use MRST2004 parton distributions [32], with densities and α_s evaluated at each corresponding order (i.e., we use $(n+1)$ -loop α_s at $N^n\text{LO}$, with $n = 0, 1, 2$). Unless stated otherwise, renormalization and factorization scales are set to their default values, $\mu_R = \mu_F = M_H$. We remind the reader that the calculation is done in the $M_t \rightarrow \infty$ limit. As for the electroweak couplings, we use the scheme where the input parameters are G_F , M_Z , M_W and $\alpha(M_Z)$. In particular we take $G_F = 1.16639 \times 10^{-5} \text{ GeV}^{-2}$, $M_Z = 91.188 \text{ GeV}$, $M_W = 80.419 \text{ GeV}$ and $\alpha(M_Z) = 1/128.89$. The decay matrix elements are implemented at Born level and the Higgs boson is treated in the narrow-width approximation. In the W and Z decays we take into account finite width effects, by using $\Gamma_W = 2.06 \text{ GeV}$ and $\Gamma_Z = 2.49 \text{ GeV}$. As far as jets are concerned, we use the k_T -algorithm [33] with jet size $D = 0.4$.

3.2 $H \rightarrow WW \rightarrow l\nu l\nu$

We consider the production of a Higgs boson with mass $M_H = 165 \text{ GeV}$. The width is computed with the program HDECAY [34] to be $\Gamma_H = 0.255 \text{ GeV}$. With this choice of M_H the Higgs boson decays almost entirely into WW pairs. We consider the decay $W \rightarrow l\nu$ by assuming only one final state lepton combination. The corresponding inclusive cross sections are given in Table 1. The NLO and NNLO K -factors are 1.84 and 2.21, respectively, and are in good agreement with the inclusive K -factors from the calculation of the total NLO and NNLO cross section [10, 11, 12].

$\sigma \text{ (fb)}$	LO	NLO	NNLO
$\mu_F = \mu_R = M_H/2$	136.37 ± 0.09	241.59 ± 0.43	268.7 ± 1.8
$\mu_F = \mu_R = M_H$	112.08 ± 0.07	206.46 ± 0.33	247.2 ± 1.3
$\mu_F = \mu_R = 2M_H$	92.88 ± 0.06	178.43 ± 0.25	227.4 ± 0.8

Table 1: *Cross sections for $pp \rightarrow H + X \rightarrow WW + X \rightarrow l\nu l\nu + X$ at the LHC when no cuts are applied.*

We first apply a set of *preselection* cuts taken from the study of Ref. [35].

1. The event should contain two leptons of opposite charge having p_T larger than 20 GeV and rapidity $|y| < 2$;
2. The missing p_T of the event should be larger than 20 GeV;
3. The invariant mass of the charged leptons should be smaller than 80 GeV;
4. The azimuthal separation of the charged leptons in the transverse plane ($\Delta\phi$) should be smaller than 135° .

The first cut selects dilepton events originating from the decay of W or Z bosons. Lepton pairs originating from the inclusive production of a Z boson are mostly rejected with cuts 2-4. The corresponding cross sections are given in Table 2. Comparing with Table 1 we find that the

σ (fb)	LO	NLO	NNLO
$\mu_F = \mu_R = M_H/2$	64.03 ± 0.06	113.57 ± 0.28	124.75 ± 1.28
$\mu_F = \mu_R = M_H$	53.10 ± 0.05	97.30 ± 0.21	116.24 ± 0.81
$\mu_F = \mu_R = 2M_H$	44.32 ± 0.04	84.69 ± 0.16	106.48 ± 0.61

Table 2: *Cross sections for $pp \rightarrow H + X \rightarrow WW + X \rightarrow \nu\bar{\nu}\nu + X$ at the LHC when preselection cuts are applied.*

efficiency is 47% both at NLO and at NNLO. The corresponding NLO and NNLO K -factors are 1.83 and 2.19. With respect to the inclusive case, we notice that the preselection cuts do not alter significantly the convergence of the perturbative expansion.

For each event, we classify the transverse momenta of the charged leptons according to their minimum and maximum value, $p_{T\min}$ and $p_{T\max}$. In Fig. 1 we plot the $p_{T\min}$ and $p_{T\max}$ distribution at LO, NLO and NNLO. We see that QCD corrections tend to make the distributions harder. This can be also appreciated from Fig. 2, where we compare the NNLO distributions with the NLO ones, normalized to the same area.

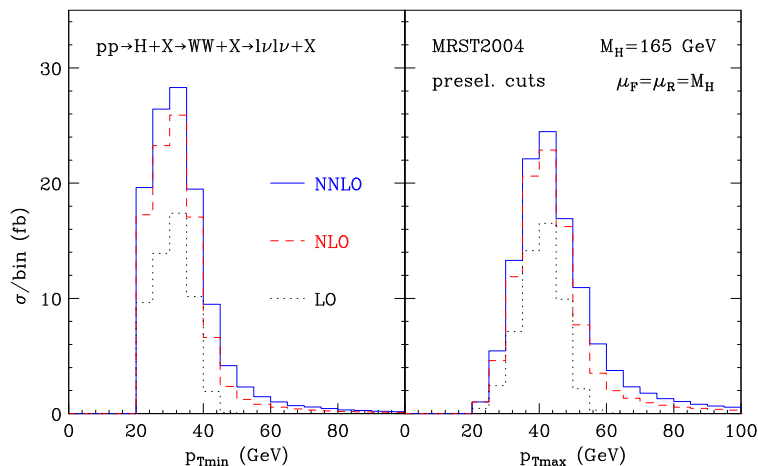


Figure 1: *Transverse momentum spectra of the charged leptons for $pp \rightarrow H + X \rightarrow WW + X \rightarrow \nu\bar{\nu}\nu + X$ at LO (dots), NLO (dashes) and NNLO (solid). Preselection cuts are applied.*

In Fig. 3 we plot the $\Delta\phi$ distribution at LO, NLO and NNLO. As is well known [36], for the Higgs boson signal the leptons tend to be close in angle, and thus most of the events are concentrated at small $\Delta\phi$. We notice that the steepness of the distribution increases when going from LO to NLO and from NLO to NNLO. As a consequence, the efficiency of a cut on this variable also increases with the perturbative order.

We finally consider the following *selection* cuts [35], which are designed to isolate the Higgs boson signal:

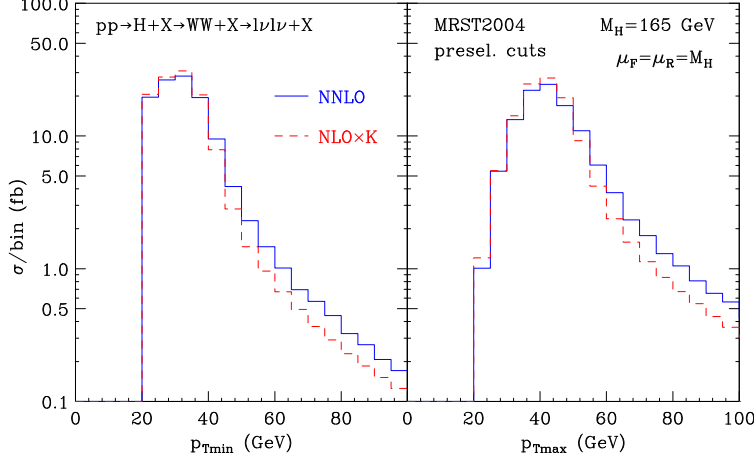


Figure 2: As in Fig. 1: comparison of p_T spectra at NNLO (solid) with NLO normalized to the same area (dashes).

1. The two charged leptons, with rapidity $|y| < 2$, should fulfil $p_{T\min} > 25$ GeV and $35 \text{ GeV} < p_{T\max} < 50$ GeV;
2. The missing p_T of the event should be larger than 20 GeV;
3. The invariant mass of the charged leptons should be smaller than 35 GeV;
4. The azimuthal separation of the charged leptons in the transverse plane ($\Delta\phi$) should be smaller than 45° ;
5. Finally, there should be no jets with p_T^{jet} larger than a given value p_T^{veto} .

These cuts further exploit: *i*) the shape of the $p_{T\min}$ and $p_{T\max}$ distributions shown in Fig. 1; *ii*) the strong angular correlations of the charged leptons leading to the steep $\Delta\phi$ distribution in Fig. 3; *iii*) The fact that the decay of top quarks from the $t\bar{t}$ background produces b -jets with large transverse momentum. A jet veto is thus very efficient to suppress this background.

In Table 3 we report the corresponding cross sections in the case of $p_T^{\text{veto}} = 30$ GeV.

σ (fb)	LO	NLO	NNLO
$\mu_F = \mu_R = M_H/2$	17.36 ± 0.02	18.11 ± 0.08	15.70 ± 0.32
$\mu_F = \mu_R = M_H$	14.39 ± 0.02	17.07 ± 0.06	15.99 ± 0.23
$\mu_F = \mu_R = 2M_H$	12.00 ± 0.02	15.94 ± 0.05	15.68 ± 0.20

Table 3: Cross sections for $pp \rightarrow H + \rightarrow WW + X \rightarrow l\nu l\nu + X$ at the LHC when selection cuts are applied and $p_T^{\text{veto}} = 30$ GeV.

A comparison with Table 2 reveals that the cross section is strongly suppressed with respect to the case in which only preselection cuts are applied: the efficiency turns out to be 8% at NLO and 6% at NNLO. The scale dependence of the result is strongly reduced at NNLO, being of

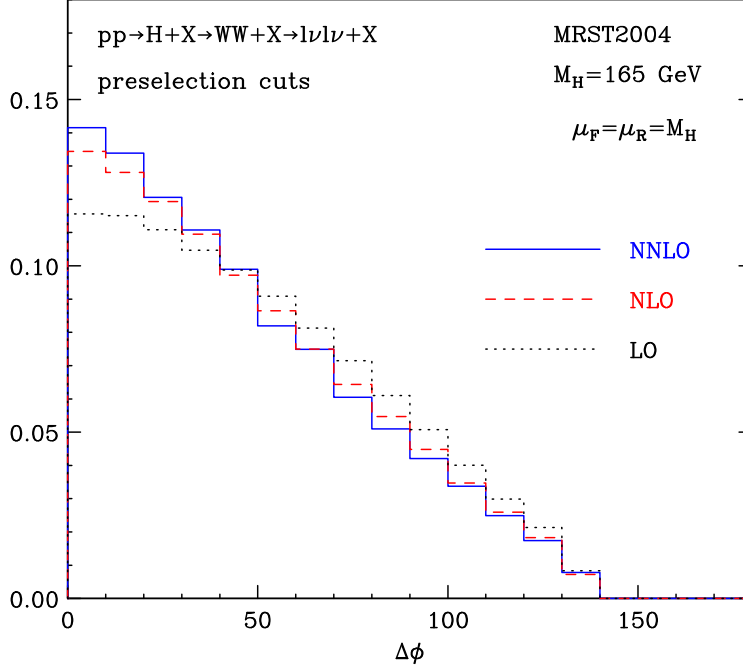


Figure 3: *Normalized distribution in the variable $\Delta\phi$ when preselection cuts are applied.*

the order of the error from the numerical integration. The impact of higher order corrections is also drastically changed. The K -factor is now 1.19 at NLO and 1.11 at NNLO. As expected, the jet veto tends to stabilize the perturbative expansion. The latter point has a simple qualitative explanation [13].

It is well known that the effect of higher order contributions to the inclusive Higgs production cross section is large. The dominant part of this effect is due to soft and virtual contributions. The characteristic scale of the highest transverse momentum p_T^{\max} of the accompanying jets is indeed $p_T^{\max} \sim \langle 1 - z \rangle M_H$, where $z = M_H^2/\hat{s}$ and $\langle 1 - z \rangle$ measures the average distance from the partonic threshold. As a consequence, the effect of the jet veto is small unless p_T^{veto} is substantially smaller than p_T^{\max} . Decreasing p_T^{veto} , the enhancement of the inclusive cross section due to soft-radiation at higher orders is reduced, and the jet veto improves the convergence of the perturbative series. Note, however, that when p_T^{veto} is much smaller than the characteristic scale $p_T^{\max} \sim \langle 1 - z \rangle M_H$, the coefficients of the perturbative series contain logarithmically enhanced contributions that may invalidate the convergence of the fixed order expansion.

In order to estimate the perturbative uncertainties affecting our calculation, in Fig. 4 we report the LO, NLO and NNLO bands as a function of p_T^{veto} , when all the other selection cuts are applied. The bands are obtained by varying $\mu_F = \mu_R$ between $M_H/2$ and $2M_H$. The results of Fig. 4 deserve some discussion.

At LO there are no jets accompanying the Higgs boson, and thus the cross section is independent on p_T^{veto} . The NLO band overlaps with the LO one for p_T^{veto} smaller than about 50 GeV. Without jet veto ($p_T^{\text{veto}} \rightarrow \infty$) the K -factor, defined with respect to the LO cross section at central values of the scales, ranges between 1.32 ($\mu_F = \mu_R = 2M_H$) and 1.63 ($\mu_F = \mu_R = M_H/2$). Comparing with the inclusive results, we see that the selection cuts 1-4 alone already imply a

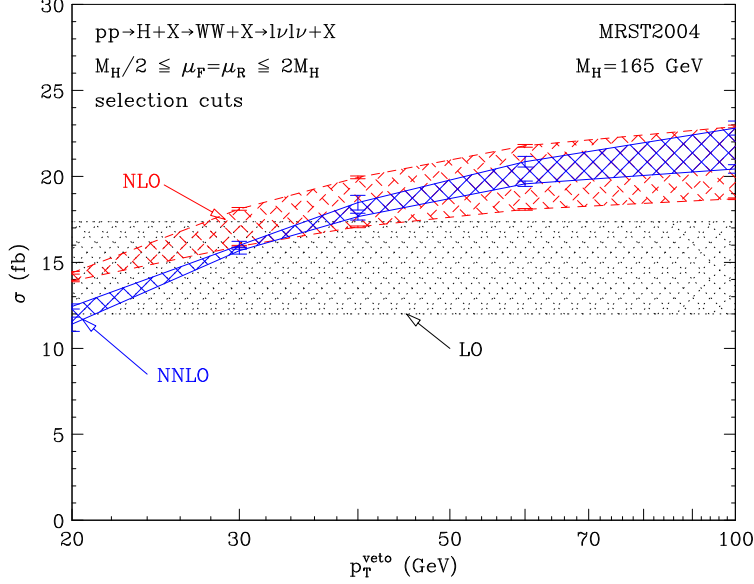


Figure 4: Cross sections as a function of p_T^{veto} when selection cuts are applied. The bands are obtained by varying $\mu_R = \mu_F$ between $M_H/2$ and $2M_H$.

reduction of the impact of higher order corrections. We also observe that the NLO band becomes very narrow as soon as p_T^{veto} decreases.

The NNLO band overlaps with the NLO one for $p_T^{\text{veto}} \gtrsim 30$ GeV and thus suggests a good convergence of the perturbative expansion in this region of p_T^{veto} . On the contrary, for $p_T^{\text{veto}} \lesssim 30$ GeV, the NNLO band is very narrow and does not overlap with the NLO one, suggesting that, in this region, the perturbative uncertainty obtained through scale variations is likely to be underestimated.

The NNLO corrections to the $pp \rightarrow H + X \rightarrow WW + X \rightarrow l\nu l\nu + X$ at the LHC were independently computed in Ref. [15]. The preselection cuts we use are the same as those considered in Ref. [15]. Taking into account the different normalization[‡], the ensuing cross sections in Table 2 are in good agreement with those given in Table 2 of Ref. [15]. When selection cuts are applied, a direct comparison is not possible, since the cuts we employ are not exactly the same. Fig. 1 of Ref. [15] shows that, when only the jet veto is applied, the NLO and NNLO bands computed as in Fig. 4 overlap for $p_T^{\text{veto}} \lesssim 40$ GeV. Nonetheless, when all the selection cuts are applied and $p_T^{\text{veto}} = 25$ GeV, the NLO and NNLO results reported in Table 3 of Ref. [15] do not overlap. Although the selection cuts we use are not exactly the same, the latter result is consistent with the behaviour we observe in Fig. 4. In the recent study of Ref. [37] the efficiencies obtained at NNLO are shown to be in good agreement with those predicted by the MC@NLO event generator [38].

[‡]In our calculation we strictly apply the large- M_t approximation, whereas in the calculation of Ref. [15] the results are normalized to the Born cross section with exact top-quark mass dependence.

3.3 $H \rightarrow ZZ \rightarrow e^+e^-e^+e^-$

We now consider the production of a Higgs boson with mass $M_H = 200$ GeV. The width is computed with the program HDECAY [34] to be $\Gamma_H = 1.43$ GeV. In this mass region the dominant decay mode is $H \rightarrow ZZ \rightarrow 4l$, providing a clean four lepton signature. In the following we consider the decay of the Higgs boson in two identical lepton pairs. When no cuts are applied, the signal cross sections are reported in Table 4. We find that the interference contribution is smaller than 1% in this mass region. The ensuing inclusive cross section is thus a factor of 2 smaller than the cross section in the decay channel $H \rightarrow ZZ \rightarrow \mu^+\mu^-e^+e^-$ [§].

σ (fb)	LO	NLO	NNLO
$\mu_F = \mu_R = M_H/2$	2.457 ± 0.001	4.387 ± 0.006	4.90 ± 0.03
$\mu_F = \mu_R = M_H$	2.000 ± 0.001	3.738 ± 0.004	4.52 ± 0.02
$\mu_F = \mu_R = 2M_H$	1.642 ± 0.001	3.227 ± 0.003	4.14 ± 0.01

Table 4: *Cross sections for $pp \rightarrow H + X \rightarrow ZZ + X \rightarrow e^+e^-e^+e^- + X$ at the LHC when no cuts are applied.*

The NLO K -factor is $K = 1.87$ whereas at NNLO we have $K = 2.26$. These results are in good agreement with those obtained from the calculation of the total NLO and NNLO cross section [10, 11, 12].

We consider the following cuts [3]:

1. For each event, we order the transverse momenta of the leptons from the largest (p_{T1}) to the smallest (p_{T4}). They are required to fulfil the following thresholds:
 $p_{T1} > 30$ GeV $p_{T2} > 25$ GeV $p_{T3} > 15$ GeV $p_{T4} > 7$ GeV ;
2. Leptons should be central: $|y| < 2.5$;
3. Leptons should be isolated: the total transverse energy E_T in a cone of radius 0.2 around each lepton should fulfil $E_T < 0.05 p_T$;
4. For each possible e^+e^- pair, the closest (m_1) and next-to-closest (m_2) to M_Z are found. Then m_1 and m_2 are required to be $81 \text{ GeV} < m_1 < 101 \text{ GeV}$ and $40 \text{ GeV} < m_2 < 110 \text{ GeV}$.

These cuts are designed to maximize the statistical significance for an early discovery, but to keep the possibility for a more detailed analysis of the properties of the Higgs boson. The corresponding cross sections are reported in Table 5.

Comparing with Table 4, we see that, contrary to what happens in the $H \rightarrow WW \rightarrow l\nu l\nu$ decay mode, the cuts are quite mild, the efficiency being 63% at NLO and 62% at NNLO. The NLO and NNLO K -factors are 1.87 and 2.22, respectively. Comparing with the inclusive case, we

[§]In the case of $H \rightarrow ZZ \rightarrow e^+e^-e^+e^-$ there is an additional diagram, obtained for example by exchanging the momenta of the two electrons, but there is also a symmetry factor 1/4, due to the two pairs of identical particles [39].

σ (fb)	LO	NLO	NNLO
$\mu_F = \mu_R = M_H/2$	1.541 ± 0.002	2.764 ± 0.005	3.013 ± 0.023
$\mu_F = \mu_R = M_H$	1.264 ± 0.001	2.360 ± 0.003	2.805 ± 0.015
$\mu_F = \mu_R = 2M_H$	1.047 ± 0.001	2.044 ± 0.003	2.585 ± 0.010

Table 5: *Cross sections for $pp \rightarrow H + X \rightarrow ZZ + X \rightarrow e^+e^-e^+e^- + X$ at the LHC when cuts are applied.*

conclude that these cuts do not change significantly the impact of QCD radiative corrections. We also find that the effect of lepton isolation is mild: at NNLO it reduces the accepted cross section by about 4%.

In Fig. 5 we plot the p_T spectra of the final state leptons. We note that at LO, without cuts, the p_{T1} and p_{T2} are kinematically bounded by $M_H/2$, whereas $p_{T3} < M_H/3$ and $p_{T4} < M_H/4$. It is well known that, in the vicinity of kinematical boundaries, QCD cross sections may develop perturbative instabilities beyond a given order, if the behaviour of the cross section is not smooth at that order [40]. This is what can be observed in the p_T spectra of the photons in the $H \rightarrow \gamma\gamma$ decay mode [16]. In the present case, the effect of the cuts further reduces the kinematically allowed region, but the LO distributions smoothly reach their kinematical boundary, and we do not observe such perturbative instabilities beyond LO.

As in Fig. 1, in Fig. 5 we see that QCD corrections tend to make the distributions harder. This can be also appreciated from Fig. 6, where we compare the NNLO distributions with the NLO ones, normalized to the same area.

4 Summary

We have presented a calculation of the NNLO cross section for Higgs boson production at the LHC, in the decay modes $H \rightarrow WW \rightarrow l\nu l\nu$ and $H \rightarrow ZZ \rightarrow 4$ leptons. The calculation takes into account all the experimental cuts designed to isolate the Higgs boson signal [3, 35]. In the case of the decay mode $H \rightarrow WW \rightarrow l\nu l\nu$, we confirm previous findings that the effect of radiative corrections is strongly reduced by the selection cuts. In the case of the decay mode $H \rightarrow ZZ \rightarrow 4$ leptons, we find that the proposed cuts are mild and do not change dramatically the size of QCD radiative corrections.

Our calculation is implemented in the numerical program HNNLO [31]. The present version of the program includes the most relevant decay modes of the Higgs boson, namely, $H \rightarrow \gamma\gamma$, $H \rightarrow WW \rightarrow l\nu l\nu$ and $H \rightarrow ZZ \rightarrow 4$ leptons. In the latter case it is possible to choose between $H \rightarrow ZZ \rightarrow \mu^+\mu^-e^+e^-$ and $H \rightarrow ZZ \rightarrow e^+e^-e^+e^-$, which includes the appropriate interference contribution. The user can apply all the required cuts on the final state leptons (photons) and the associated jets and plot the corresponding distributions in the form of bin histograms. These features should make our program a useful tool for Higgs studies at the Tevatron and the LHC.

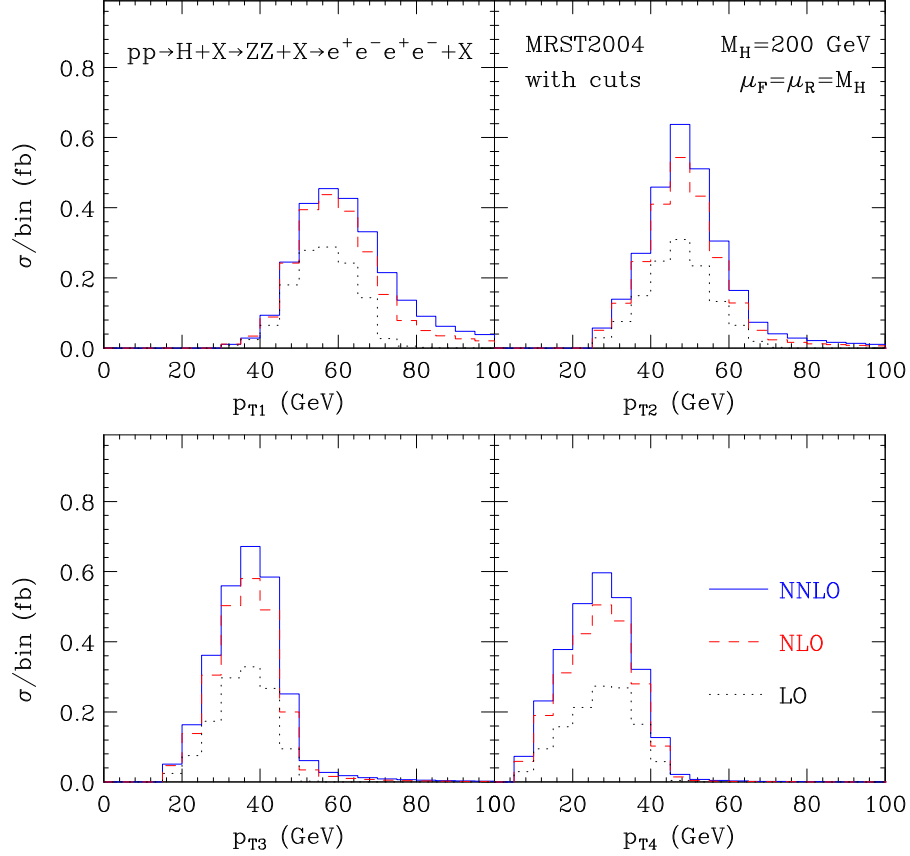


Figure 5: *Transverse momentum spectra of the final state leptons for $pp \rightarrow H + X \rightarrow ZZ + X \rightarrow e^+e^-e^+e^- + X$, ordered according to decreasing p_T , at LO (dotted), NLO (dashed), NNLO (solid).*

Acknowledgements

I wish to thank Stefano Catani for helpful discussions and comments.

References

- [1] For a review on Higgs physics in and beyond the Standard Model, see J. F. Gunion, H. E. Haber, G. L. Kane and S. Dawson, *The Higgs Hunter's Guide* (Addison-Wesley, Reading, Mass., 1990); A. Djouadi, report LPT-ORSAY-05-17 [hep-ph/0503172], report LPT-ORSAY-05-18 [hep-ph/0503173].
- [2] ATLAS Coll., *ATLAS Detector and Physics Performance: Technical Design Report*, Vol. 2, report CERN/LHCC/99-15 (1999).
- [3] CMS Coll., *CMS Physics Technical Design Report: Physics Performance*, Vol. 2, report CERN/LHCC/2006-021 (2006).
- [4] S. Dawson, Nucl. Phys. B **359** (1991) 283.

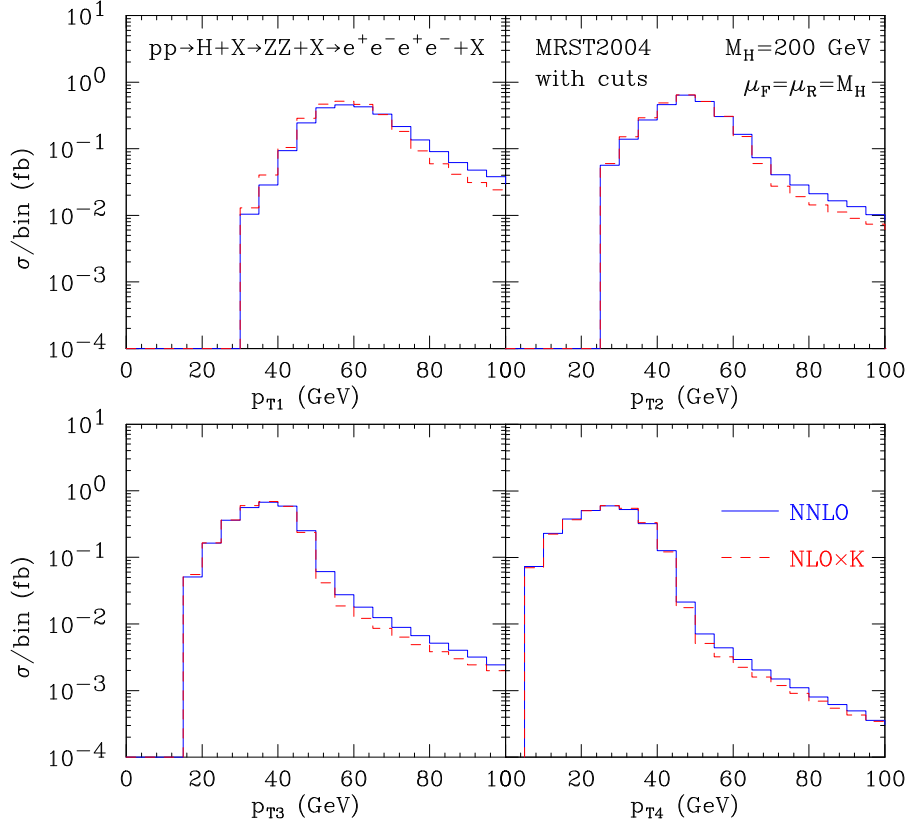


Figure 6: *As in Fig. 5: comparison of lepton p_T spectra at NNLO (solid) with NLO normalized to the same area (dashes).*

- [5] A. Djouadi, M. Spira and P. M. Zerwas, Phys. Lett. B **264** (1991) 440.
- [6] M. Spira, A. Djouadi, D. Graudenz and P. M. Zerwas, Nucl. Phys. B **453** (1995) 17.
- [7] R. V. Harlander, Phys. Lett. B **492** (2000) 74.
- [8] S. Catani, D. de Florian and M. Grazzini, JHEP **0105** (2001) 025.
- [9] R. V. Harlander and W. B. Kilgore, Phys. Rev. D **64** (2001) 013015.
- [10] R. V. Harlander and W. B. Kilgore, Phys. Rev. Lett. **88** (2002) 201801.
- [11] C. Anastasiou and K. Melnikov, Nucl. Phys. B **646** (2002) 220.
- [12] V. Ravindran, J. Smith and W. L. van Neerven, Nucl. Phys. B **665** (2003) 325.
- [13] S. Catani, D. de Florian and M. Grazzini, JHEP **0201** (2002) 015.
- [14] C. Anastasiou, K. Melnikov and F. Petriello, Phys. Rev. Lett. **93** (2004) 262002, Nucl. Phys. B **724** (2005) 197.
- [15] C. Anastasiou, G. Dissertori and F. Stockli, JHEP **0709** (2007) 018.
- [16] S. Catani and M. Grazzini, Phys. Rev. Lett. **98** (2007) 222002.

- [17] R. K. Ellis, D. A. Ross and A. E. Terrano, Nucl. Phys. B **178** (1981) 421.
- [18] S. Frixione, Z. Kunszt and A. Signer, Nucl. Phys. B **467** (1996) 399; S. Frixione, Nucl. Phys. B **507** (1997) 295.
- [19] S. Catani and M. H. Seymour, Nucl. Phys. B **485** (1997) 291 [Erratum-ibid. B **510** (1997) 503].
- [20] D. A. Kosower, Phys. Rev. D **57** (1998) 5410, Phys. Rev. D **67** (2003) 116003, Phys. Rev. D **71** (2005) 045016.
- [21] S. Weinzierl, JHEP **0303** (2003) 062, JHEP **0307** (2003) 052.
- [22] S. Frixione and M. Grazzini, JHEP **0506** (2005) 010.
- [23] A. Gehrmann-De Ridder, T. Gehrmann and E. W. N. Glover, Phys. Lett. B **612** (2005) 36, Phys. Lett. B **612** (2005) 49, JHEP **0509** (2005) 056; A. Daleo, T. Gehrmann and D. Maitre, JHEP **0704** (2007) 016.
- [24] G. Somogyi, Z. Trocsanyi and V. Del Duca, JHEP **0506** (2005) 024, JHEP **0701** (2007) 070; G. Somogyi and Z. Trocsanyi, JHEP **0701** (2007) 052.
- [25] A. Gehrmann-De Ridder, T. Gehrmann and E. W. N. Glover, Nucl. Phys. B **691** (2004) 195.
- [26] S. Weinzierl, Phys. Rev. D **74** (2006) 014020.
- [27] A. Gehrmann-De Ridder, T. Gehrmann, E. W. N. Glover and G. Heinrich, Phys. Rev. Lett. **99** (2007) 132002.
- [28] A. Gehrmann-De Ridder, T. Gehrmann, E. W. N. Glover and G. Heinrich, JHEP **0711** (2007) 058.
- [29] A. Gehrmann-De Ridder, T. Gehrmann, E. W. N. Glover and G. Heinrich, JHEP **0712** (2007) 094.
- [30] J. Campbell, R.K. Ellis, *MCFM - Monte Carlo for FeMtobarn processes*, <http://mcfm.fnal.gov>
- [31] <http://theory.fi.infn.it/grazzini/codes.html>
- [32] A. D. Martin, R. G. Roberts, W. J. Stirling and R. S. Thorne, Phys. Lett. B **604** (2004) 61.
- [33] S. Catani, Y. L. Dokshitzer, M. H. Seymour and B. R. Webber, Nucl. Phys. B **406** (1993) 187; S. D. Ellis and D. E. Soper, Phys. Rev. D **48** (1993) 3160.
- [34] A. Djouadi, J. Kalinowski and M. Spira, Comput. Phys. Commun. **108** (1998) 56.
- [35] G. Davatz, G. Dissertori, M. Dittmar, M. Grazzini and F. Pauss, JHEP **0405** (2004) 009.
- [36] M. Dittmar and H. K. Dreiner, Phys. Rev. D **55** (1997) 167.
- [37] C. Anastasiou, G. Dissertori, F. Stoeckli and B. R. Webber, report ETHZ-IPP/PR-2008-01, arXiv:0801.2682 [hep-ph].

- [38] S. Frixione and B. R. Webber, JHEP **0206** (2002) 029; S. Frixione, P. Nason and B. R. Webber, JHEP **0308** (2003) 007.
- [39] C. Zecher, T. Matsuura and J. J. van der Bij, Z. Phys. C **64** (1994) 219.
- [40] S. Catani and B. R. Webber, JHEP **9710** (1997) 005.